Journal of Dental Research
2019, Vol. 98(1) 54–60

DOI: 10.1177/0022034518798810
journals.sagepub.com/home/jdr

The Mutational Profile of Unicystic Ameloblastoma

K. Heikinheimo[1], J.-M. Huhtala[1], A. Thiel[2], K.J. Kurppa[3], H. Heikinheimo[4], M. Kovac[5], C. Kragelund[6], G. Warfvinge[7], H. Dawson[8], K. Elenius[3], A. Ristimäki[2,9], D. Baumhoer[5*], and P.R. Morgan[10*]

Abstract

BRAF V600E is the most common mutation in conventional ameloblastoma (AM) of the mandible. In contrast, maxillary AMs appear to harbor more frequently *RAS, FGFR2*, or *SMO* mutations. Unicystic ameloblastoma (UAM) is considered a less aggressive variant of ameloblastoma, amenable to more conservative treatment, and classified as a distinct entity. The aim of this study was to characterize the mutation profile of UAM ($n = 39$) and to compare it to conventional AM ($n = 39$). The associations between mutation status and recurrence probability were also analyzed. In the mandible, 94% of UAMs (29/31, including 8/8 luminal, 6/8 intraluminal, and 15/15 mural subtypes) and 74% of AMs (28/38) revealed *BRAF* V600E mutations. Among the *BRAF* wild-type cases, 1 UAM showed a missense SMO mutation (p.L412F), whereas 2 NRAS (p.Q61R), 2 HRAS (p.Q61R), and 2 FGFR2 (p.C383R) activating mutations were identified in AM. Of the 3 maxillary UAMs, only 1 revealed a *BRAF* V600E mutation. Taken together, our findings demonstrate high frequency of activating *BRAF* V600E mutations in both UAM and AM of the mandible. In maxillary UAMs, the *BRAF* V600E mutation prevalence appears to be lower as was shown for AM previously. It could therefore be argued that UAM and AM are part of the spectrum of the same disease. AMs without *BRAF* V600E mutations were associated with an increased rate of local recurrence ($P = 0.0003$), which might indicate that routine mutation testing also has an impact on prognosis.

Keywords: drug therapy, genetic markers, odontogenic tumors, mitogen-activated protein kinase kinases, jaw neoplasms, survival analysis

Introduction

Four years ago, we reported *BRAF* V600E mutations in 63% (15/24) of conventional ameloblastomas (AMs), introducing aberrant MAP-kinase signaling as underlying the majority of AMs (Kurppa et al. 2014; Heikinheimo, Kurppa, and Elenius 2015). We also demonstrated that *BRAF* mutation-negative nonimmortalized primary AM cells were sensitive to epidermal growth factor receptor (EGFR)–targeted drugs. These observations suggested that 2 groups of AM patients exist: *BRAF* mutation-negative patients who might benefit from EGFR inhibition and *BRAF* mutation-positive patients who could potentially benefit from BRAF-targeted therapies (Gomes et al. 2014; Heikinheimo, Kurppa, and Elenius 2015). Brown and colleagues (2014) also found that *BRAF* wild-type tumors recur more rapidly.

In addition to the high incidence of activating *BRAF* mutations, mutually exclusive and less common mutations in other MAP-kinase genes such as *KRAS, NRAS*, and *HRAS* and *FGFR2* have been reported in AM (Brown et al. 2014; Sweeney et al. 2014). These genes mediate cell proliferation, differentiation, and survival and are commonly activated in various human malignancies (Holderfield et al. 2014). In addition to mutations in the MAP-kinase cascade, a high incidence of activating mutations in the *SMO* gene has been reported in AM, particularly in maxillary tumors (Brown et al. 2014; Sweeney et al. 2014). SMO is a transmembrane activator of the hedgehog signaling pathway, which is commonly mutated in basal cell carcinoma and occasionally in odontogenic keratocyst (Kim et al. 2013). Rarely detected mutations in AM include *PIK3CA, SMARCB1*, and *CTNNB1* (Brown et al. 2014; Sweeney et al. 2014).

[1]Department of Oral and Maxillofacial Surgery, Institute of Dentistry, University of Turku and Turku University Hospital, Finland
[2]Genome-Scale Biology, Research Programs Unit, University of Helsinki, Helsinki, Finland
[3]Department of Medical Biochemistry and Genetics and MediCity Research Laboratories, University of Turku, Turku, Finland
[4]Chief Chief Technologies, Helsinki, Finland
[5]Bone Tumour Reference Centre at the Institute of Pathology, University Hospital Basel and University of Basel, Basel, Switzerland
[6]Department of Oral Pathology and Medicine, Copenhagen, Denmark
[7]Department of Oral Pathology, Malmö University, Malmö, Sweden
[8]Institute of Pathology, University of Bern, Bern, Switzerland
[9]Department of Pathology, HUSLAB, Helsinki University Central Hospital, and Medicum, University of Helsinki, Finland
[10]Head & Neck Pathology, King's College London, Guy's Hospital, London, UK
*Authors contributing equally to this study.

A supplemental appendix to this article is available online.

Corresponding Author:
K. Heikinheimo, Department of Oral and Maxillofacial Surgery, Institute of Dentistry, University of Turku, Lemminkäisenkatu 2, FI-20520 Turku, Finland.
Email: krihei@utu.fi

While AM represents a benign but locally aggressive odontogenic neoplasm that can recur following incomplete excision, the unicystic subtype, unicystic ameloblastoma (UAM), remains a matter of ongoing debate (Wright et al. 2014). The current World Health Organization (WHO) Classification of Head and Neck Tumors (2017) concurs with the original description of UAM as representing a prognostically distinct entity comprising 3 distinct subtypes: luminal, intraluminal, and mural (Robinson and Martinez 1977; Vered et al. 2017). The luminal and intraluminal UAM variants are generally regarded as the least aggressive form, whereas the mural type seems to recur at similar rates to AM. Hence, some experts regard it as an early version of AM (Li et al. 2000; Wright et al. 2014).

While the mutational profile of AM has been analyzed intensively, there are few data on the molecular background of UAM (Diniz et al. 2015; Pereira et al. 2016). We therefore analyzed UAMs for driver mutations and compared the results to those obtained from a similar number of AM cases. To further elucidate the clinical significance of the mutation testing, we have analyzed results for treatment modality (enucleation or resection), follow-up time (months), and outcome (recurrence or no recurrence).

Materials and Methods

Patients and Tissue Specimens

Seventy-eight formalin-fixed, paraffin-embedded (FFPE) ameloblastoma samples, consisting of 39 UAMs and 39 conventional AMs, were included in the study. These were selected after careful histopathological reevaluation by pathologists KH, PRM, CK, GW, and DB (Appendix Tables 1 and 2). The tissue blocks were collected from oral pathology and/or pathology departments in Finland, Denmark, Sweden, the United Kingdom, and Switzerland. Out of these 78 cases, fresh tumor specimens were also available from 24 AM cases as described previously (Kurppa et al. 2014). Clinical patient data (Appendix Tables 1 and 2) and follow-up information were obtained from patients' medical records (Appendix Tables 3 and 4). Approvals from the ethics committees (1/11 March 2007, 0/H0703/054 and CPP53-10) and patients' written informed consents in relation to the fresh tumor specimens were obtained in accordance with the Helsinki Declaration.

RNA and DNA Extraction

Cryosections of the fresh surgical specimens and sections from the FFPE tissue blocks were reviewed prior to RNA and DNA extraction to confirm that over 90% of the tissue represented tumor. Total RNA was isolated from fresh AM ($n=24$) tissue samples as described earlier (Heikinheimo et al. 1991). DNA was isolated from FFPE UAM ($n=39$) and AM ($n=15$ tissue samples after using the QIAamp DNA Mini Kit (Qiagen) according to the manufacturer's instructions as previously reported (Thiel et al. 2013). A flowchart of the study is given in Appendix Figure 1.

BRAF *V600E Genotyping*

Genotyping was performed as described previously (Thiel et al. 2013). Quantitative reverse transcription polymerase chain reaction (qPCR) genotyping was used to detect *BRAF* V600E mutation (NM_004333.4(BRAF)): c.1799T>A, pVal600Glu in UAM ($n=39$) and AM ($n=14$) samples. Primers and probes to detect *BRAF* wild-type and V600E have been described previously (Benlloch et al. 2006). Each sample was processed in duplicate with the 7500 Fast Real-Time PCR machine (Thermo Fisher Scientific). The total reaction volume was 10 µL per well, and the genotyping cycling conditions were 60°C for 1 min and 95°C for 10 min, followed by 40 cycles of 95°C denaturation for 15 s and 60°C annealing for 1.5 min. After 40 cycles, post-PCR reading occurred at 60°C for 1 min. Genomic DNA from HT-29 cells was used as a positive control. The delta Ct (Ct mutation – Ct wild-type; threshold 0.05) limit was 6.5, and Ct values above 36 were disregarded.

Sanger Sequencing

Twenty-four mandibular AMs were analyzed for recurrent mutations in *KRAS, NRAS*, and *HRAS* genes (codons 12, 13, and 61) by complementary DNA (cDNA) sequencing. cDNA synthesis and Sanger sequencing of *KRAS, NRAS*, and *HRAS* were performed as previously described (Kurppa et al. 2014). Sanger sequencing was also used to validate mutations identified by semiconductor sequencing.

Next-Generation Sequencing

Ion torrent semiconductor sequencing was used for the analysis of 4 UAMs (12, 13, 17, and 29) and 6 AM cases (3, 13, 16, 26, 35, and 39), respectively, in which BRAF, NRAS, or HRAS mutations were not identified (Appendix Tables 1 and 2). The Ion AmpliSeq Comprehensive Cancer Panel was used in conjunction with the AmpliSeq Library Kit 2.0 to capture exons of 143 genes from the Cancer Gene Census database, and the resulting libraries were run on the Ion PGM Sequencer. The raw reads were processed using Ion Reporter software with standard settings.

Variant Detection and Filtering

Sequence reads were mapped onto the human genome hs37d5 using the BWA software. We then used the GATK haplotype caller with standard settings, followed by variant quality score recalibration for single-base substitution identification and the Scalpel algorithm for indels. The 2017 versions of ANNOVAR databases were used for variant annotation. Clinical significance of variant calls was assessed using the consensus mutation classification criteria of the American College of Medical Genetics and Genomics and the Association for Molecular Pathology (Richards et al. 2015).

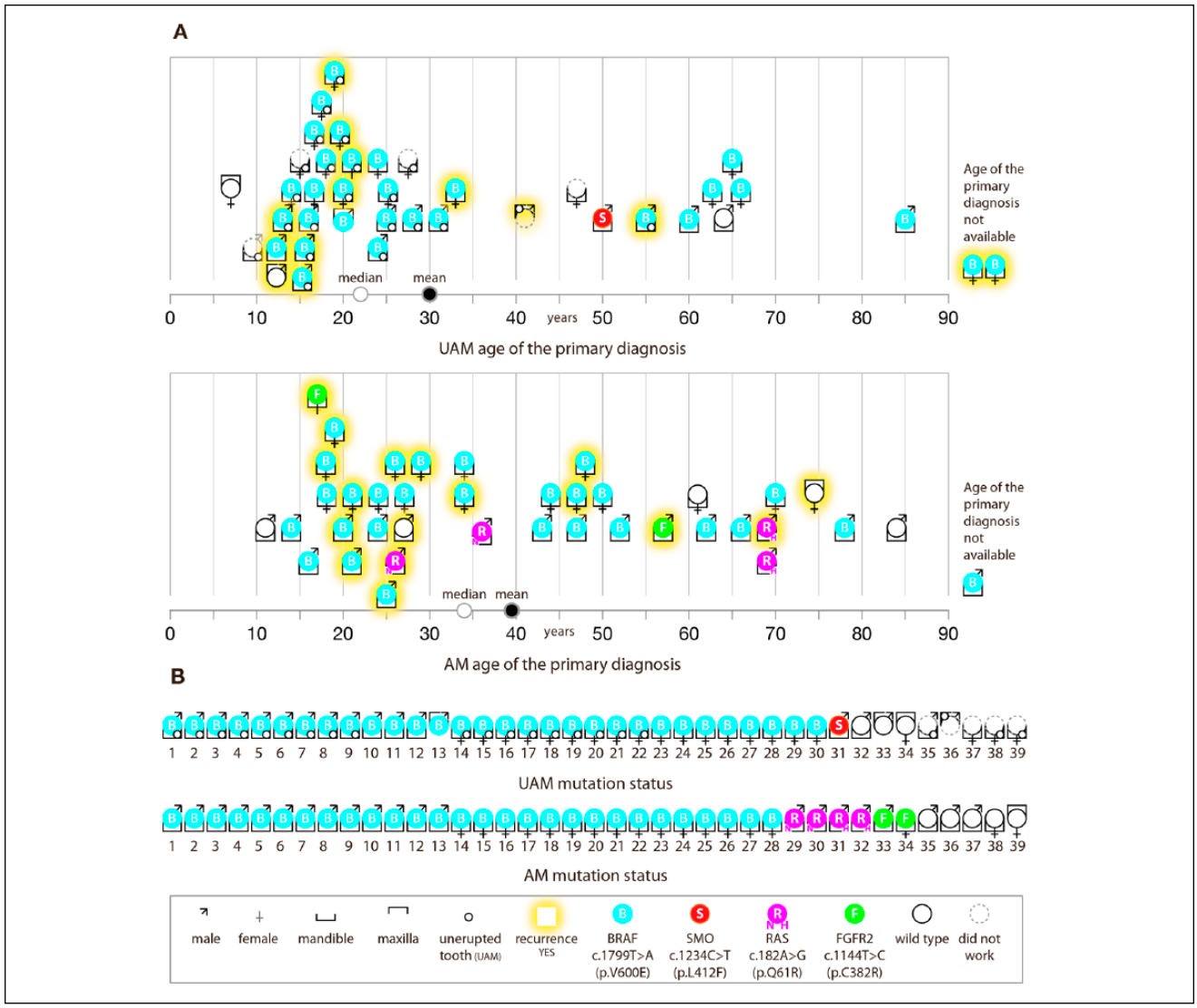

Figure 1. Oncogenic mutations in unicystic ameloblastoma (UAM) and conventional ameloblastoma (AM) samples. Interactive presentation available at www.kristiinaheikinheimo.fi/uamam. By clicking each case symbol, the patient data are shown. (**A**) Mutations in association with the clinical parameters in UAM and AM, including the age of the patient, location in mandible versus maxilla, and the connection of UAMs with an unerupted tooth. The mean and median ages at primary diagnosis of the UAM and AM patients are shown. In 2 UAM patients and 1 AM patient, the age at primary diagnosis was not available. (**B**) Thirty UAM samples were *BRAF* V600E positive as detected by genotyping. One UAM was SMO p.L412F positive as detected by targeted next-generation and Sanger sequencing. Three UAM samples were wild type, and 5 samples could not be processed because of the poor quality or insufficient amount of the DNA. Twenty-eight AM samples were BRAF V600E positive, 4 RAS Q61R positive (of which 2 were HRAS and 2 were NRAS), and 2 FGFR2 p.C382R positive by Sanger sequencing and next-generation sequencing. In 6 AM cases, no mutations were detected.

Immunohistochemistry

Mouse monoclonal antibodies to human BRAF p.V600E (clone VE1; 1:2,000) and rabbit monoclonal antibodies to human RAS p.Q61R (clone SP174; 1:50), both from Spring Bioscience, were used. Three-micron sections were cut from undecalcified FFPE blocks, processed, and stained with Ventana BenchMark XT immunostainer (Ventana Medical Systems). BRAF mutations were visualized using OptiView DAB IHCv3 (Ventana Medical Systems) and RAS mutations with UltraViewRed (Ventana Medical Systems). The sections were counterstained with hematoxylin.

Statistical Analysis

Kaplan-Meier curves (Therneau and Grambsch 2000; Rich et al. 2010) were calculated to analyze the recurrence-free survival probability in patients after treatment based on follow-up information. The Kaplan-Meier analysis was conducted using the statistical software R survival package (Therneau 2015). To establish statistical significance, the log-rank test *P* value was computed using the *survdiff* function in the R package "survival."

Kaplan-Meier analyses were carried out on 33 UAMs and 19 AMs, for which the following data were available: treatment (enucleation vs. resection), follow-up time (months), and

outcome (recurrence or no recurrence). For patients who underwent multiple treatments (8 UAMs and 7 AMs), each observation was treated as a separate data point in the analysis.

Multiple Kaplan-Meier analyses were carried out comparing 2 selected nonoverlapping groups, UAMs and AMs, in each analysis. The 2 groups were compared in relation to *BRAF* V600E versus wild type, mandible versus maxilla, and resection versus enucleation. Comparisons were made between the AM and UAM groups against each other as a whole, the mandibular AM *BRAF* V600E–positive group against the mandibular UAM *BRAF* V600E–positive group and the mandibular AM *BRAF* V600E–positive group against the mandibular mural *BRAF* V600E–positive UAMs.

Odds ratio (Bland and Altman 2000) was calculated using the Wald method to compare the likelihood of recurrence between the *BRAF* V600E and wild-type ameloblastomas using functionality provided by the statistical software R fmsb package (https://cran.r-project.org/web/packages/fmsb/). In addition to the empirical odds ratio, the 95% confidence interval (CI) and *P* value were computed.

Results

Clinical Data

The UAM and AM clinicopathological data and mutation status are summarized in Figure 1, Appendix Tables 1 and 2, and Appendix Figure 2.

In the UAM series, 21 of 39 were female and 18 of 39 were male, and in the AM series, 18 of 39 were female and 21 of 39 were male. Ninety percent (35/39) of the UAMs and 97% (38/39) of the AMs were located in the mandible. The mean age at the time of diagnosis was 29.9 y for UAM patients (range, 7–85 y) and 39.4 y for AM patients (range, 11–84 y).

Follow-up Information

Follow-up time and outcome (recurrence or no recurrence) were retrieved from the medical records of 33 of 39 UAM and 21 of 39 AM patients (Appendix Tables 3 and 4 and Appendix Fig. 2). The follow-up time was 8.2 y on average for the UAMs and 11.7 y for the AMs. Fourteen of 33 UAMs (12 in the mandible and 2 in the maxilla) and 17 of 21 AMs (16 in the mandible and 1 in the maxilla) were reported to have 1 or multiple recurrences.

The time to first recurrence information (average 6.1 y) was available for 12 of 33 UAM patients. Five represented intraluminal, 2 luminal, and 5 mural subtypes. Eleven of the primary UAMs were treated by enucleation and 1 by resection.

The time to first recurrence information (average 7.8 y) was available for 14 of 21 AM patients. Eleven represented follicular, 9 plexiform, and 1 acanthomatous subtypes. Seven of 14 of the primary AMs were treated by enucleation and 7 of 14 by resection. The first recurrence following enucleation occurred after an average of 6.2 y and that following resection after 8.6 y.

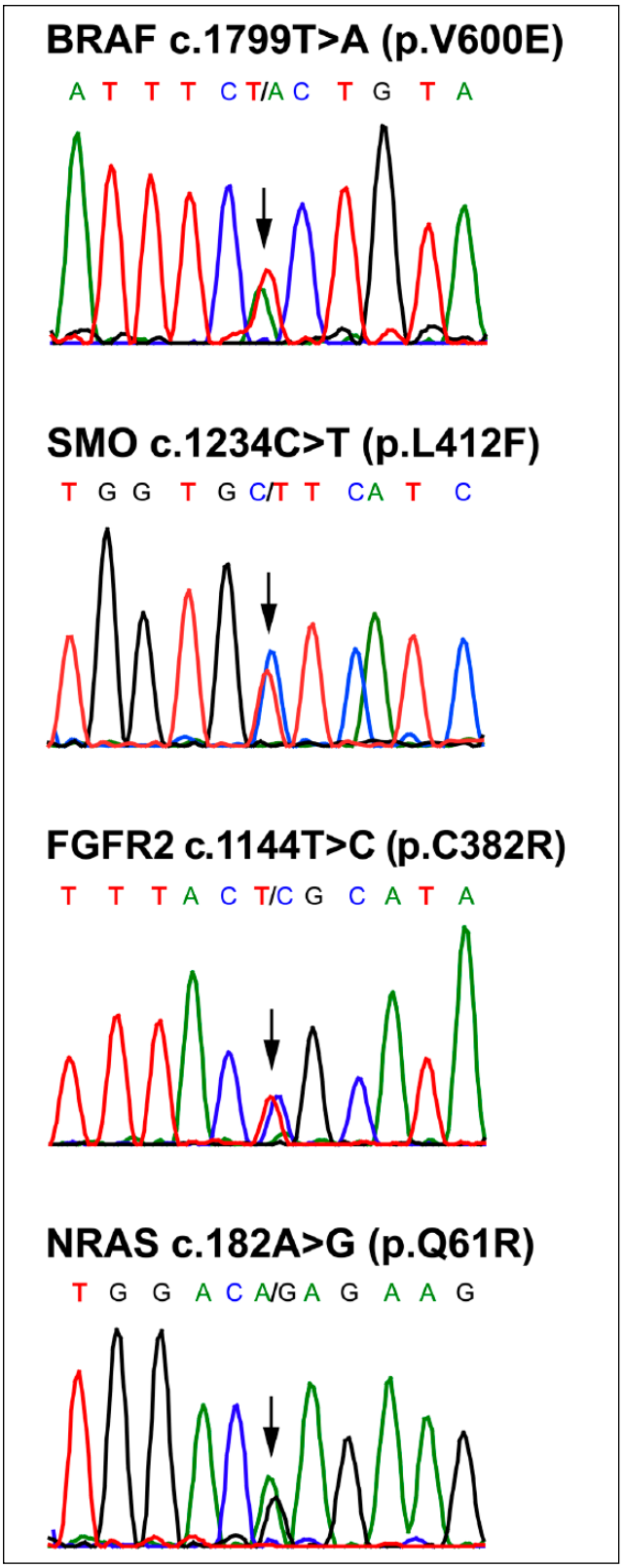

Figure 2. Sanger sequencing showing the mutated nucleotide responsible for the *BRAF* c.1799T>A (p.V600E), *SMO* c.1234C>T (p.L412F), *FGFR2* c.1144T<C (p.C382R), *NRAS* c.182A>G (p.Q61R) substitution (arrow).

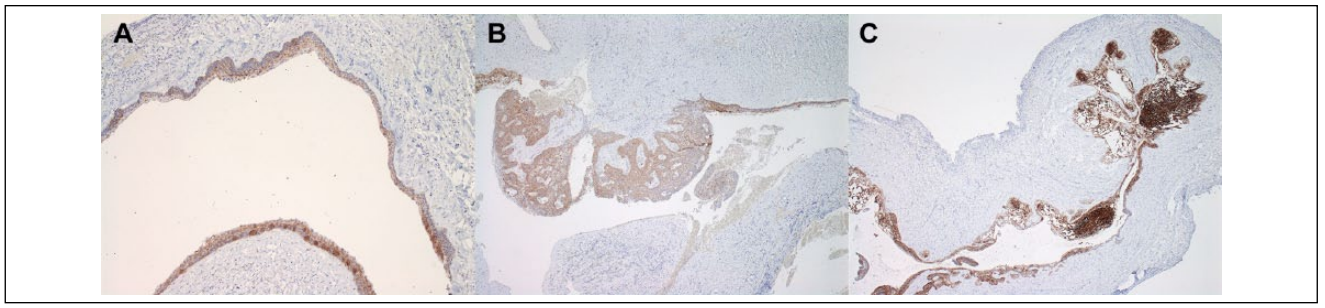

Figure 3. Immunohistochemical staining in unicystic ameloblastomas using BRAF V600E mutation-specific monoclonal antibody. (**A**) Luminal type. (**B**) Intraluminal type. (**C**) Mural type. In all variants, intracellular staining is uniform throughout the epithelium. Magnification: A = x5; B and C = x2.5.

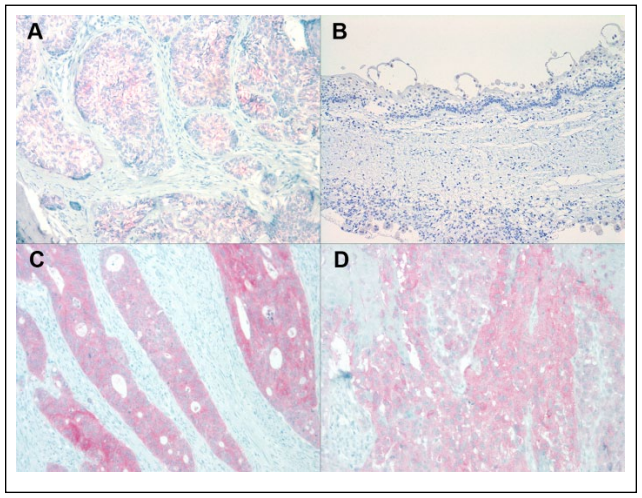

Figure 4. Immunohistochemical staining in ameloblastomas using NRAS Q61R mutation-specific rabbit monoclonal antibody. (**A**) Conventional ameloblastoma (case 19) with staining of all cells in the epithelial follicles. (**B**) Unicystic ameloblastoma, typically nonstaining. Positive control tissues: (**C**) Rectal carcinoma. (**D**) Melanoma. Magnification: A = x20; B–D = x10.

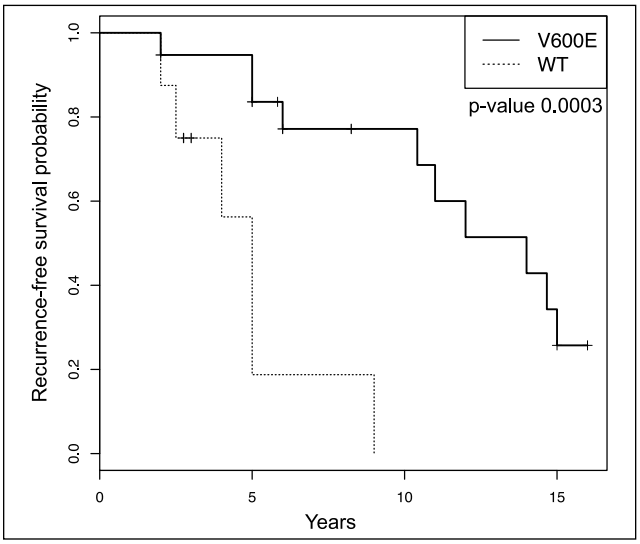

Figure 5. Recurrence-free survival probability of *BRAF* V600E–positive ($n = 12$) and *BRAF* V600E–negative ($n = 7$) conventional ameloblastomas as a function of years elapsed after last treatment.

Mutations in UAM and AM

The quality of DNA was found to be suitable for sequencing in 34 of 39 UAM and in 39 of 39 AM samples. The cancer-driving mutations detected are listed in Figure 1, Appendix/Tables 1 and 2, and Appendix/Figure 2.

In the mandible, 94% (29/31) of the UAMs were *BRAF* V600E positive: 8 of 8 luminal, 6 of 8 intraluminal, and 15 of 15 mural subtypes. In 2 mandibular intraluminal *BRAF* mutation-negative UAMs, 1 harbored a *SMO* (p. L412F) mutation, but in the other case, no mutation was identified. In the maxilla, 33% (1/3) were *BRAF* V600E positive and 67% (2/3) were *BRAF* V600E wild types.

Seventy-four percent of the mandibular AMs were *BRAF* V600E positive (28/38). In addition, 2 *NRAS* c.182A>G (5%) and 2 *HRAS* c.182A>G (5%) single-nucleotide substitutions were detected (Figs. 1 and 2). In both genes, the mutations corresponded to an amino acid substitution Q61R, which is a well-known activating mutation (Buhrman et al. 2010). Two *FGFR2* (p.C383R; 5%) mutations were detected in AM by targeted, next-generation sequencing and were further confirmed by Sanger sequencing (Figs. 1 and 2). *HRAS, BRAF*, and *FGFR2* mutations were mutually exclusive. Four mandibular AMs were *BRAF, RAS*, and *FGFR2* negative. In the maxilla, 1 AM was *BRAF* mutation negative.

Associations of BRAF *V600E Mutations with Age*

The *BRAF* V600E mutation status has been suggested to be associated with younger age in ameloblastoma patients (Brown et al. 2014). The small number of *BRAF* V600E wild-type ($n = 4$) UAMs precluded statistical analysis. For the *BRAF* V600E–positive AMs, the mean age at the time of diagnosis of the primary tumor was 36.2 y. Patients with wild-type tumors had a mean age of 47.2 y at diagnosis. We were not able to establish statistical significance between the mean ages.

Immunohistochemistry

BRAF V600E or RAS p.Q61R was scored positive when tumor cells displayed a detectable granular cytoplasmic

staining. The staining intensity was moderate to strong and relatively homogeneous (Figs. 3 and 4). Ameloblastoma patients, positive for the mutation by immunohistochemistry (IHC), were also positive for the mutation as analyzed by genetic methods (Fig. 1 and Appendix Tables 1 and 2). The only exceptions were 3 *BRAF* V600E mutation-positive AMs (cases 6, 34, and 36), which were negative with IHC, most likely because the stainings were done on decalcified tissue using formic acid, which is known to hinder detection of BRAF V600E by IHC.

Survival Analysis

A statistically significant result ($P = 0.0003$) was obtained when comparing recurrence-free survival of AM patients with ($n = 12$) and without ($n = 7$) *BRAF* V600E mutations (Fig. 5). The other Kaplan-Meier analyses did not yield statistically significant *P* values due to the small number of patients (Appendix Fig. 3). The empirical odds of recurrence of *BRAF* wild-type tumors within the AM group were twice as high as in the *BRAF* V600E group of AMs (CI, 0.17–24.1; $P = 0.2$).

Discussion

A number of unanswered questions persist regarding the diagnosis and treatment of UAM. Clinically, most patients are in their second to third decades of life at the time of initial diagnosis. Most lesions develop in a dentigerous relationship to an unerupted tooth. They are unilocular on imaging, but diagnosis is dependent on histopathological examination. This introduces another set of problems. Initial biopsy may include only the most accessible, cystic wall in which classical features of ameloblastoma may be absent. Such cases may include AM, diagnosed only after conservative excision. Most of the present UAM cases and many AMs were initially treated this way (Appendix Tables 1 and 2). Extensive sampling was performed in all UAM cases to exclude conventional AM.

In the present study, 90% (35/39) of UAMs developed in the mandible, which is in line with a previously reported Chinese cohort (91%, 30/33) (Li et al. 2000). The reason for the predilection of both UAM and AM for the mandible, as well as the differences in the prevalence of mutations found between the mandible and maxilla, is not known, but it is most likely linked to the differences in the expression of homeobox genes. These, such as *DLX* and *MSX*, are important transcription factors regulating the patterning of teeth, and their expression patterns differ in the upper and lower jaws (Thomas and Sharpe 1998).

The mean age at the primary diagnosis of UAM in the present study was 22.8 y in the case of association with an impacted tooth and 29.9 y without. In contrast, the mean age of the AM patients was 39.4 y. These findings coincide with previous data and the concept that the mean age of UAM patients is generally lower when the neoplasm is in dentigerous relationship to an unerupted tooth, most often the third molar, than without impaction (Vered et al. 2017). The reason for this is unknown, but it is most likely linked to the origin of ameloblastoma from dental lamina (Heikinheimo, Kurppa, Laiho, et al. 2015).

In a recent study, 62.5% of mandibular UAMs were reported to show *BRAF* V600E mutations as detected by TaqMan qPCR and Sanger sequencing (Pereira et al. 2016). In the present study, 94% of the mandibular UAMs revealed *BRAF* V600E mutations. In 1 *BRAF* wild-type mandibular tumor, a SMO p.L412F mutation was identified. Interestingly, Sweeney et al. (2014) reported *SMO* mutation in 1 mandibular and in 10 maxillary AMs, and Brown et al. (2014) presented 2 mandibular and 2 maxillary AMs with or without a MAP-kinase mutation. SMO p. L412F is a well-known pathogenic mutation that seems to be functionally equivalent across different tumor types (Cosmic database: Mutation ID COSM2160377).

It is of interest that the UAMs seemed to be relatively uniformly positive for the *BRAF* V600E mutations, also associated with other benign and premalignant conditions (Kato et al. 2016), whereas a few AMs also harbored other mutations. Among the *BRAF* wild-type AM cases, 2 harbored NRAS p.Q61R, 2 HRAS p.Q61R, and 2 FGFR2 p.C383R mutations. These hotspot mutations are commonly activated in various human malignancies and have also been reported in AM (Brown et al. 2014; Holderfield et al. 2014; Sweeney et al. 2014). The results of the present study show that the mutation profile of UAM appears to be more homogeneous than that of the AM, in which other MAP-kinase–related mutations such as *RAS* and *FGFR2* are also found.

BRAF wild-type AMs have been reported to be more common in the maxilla (Brown et al. 2014; Sweeney et al. 2014) and relapse earlier than the *BRAF*-mutated ones (Brown et al. 2014). In this study, a statistically significant association with an increased rate of recurrence ($P = 0.0003$) was found in the wild-type AM group compared to the *BRAF*-mutated group, as reported by Brown et al. (2014). We further evaluated the results using an odds ratio. The empirical odds ratio (2.0) showed that odds of recurrence in the BRAF wild-type group are twice as high as in the AM group, but due to the small number of patients ($n = 19$), the *P* value was not in the range of statistical significance. More ameloblastoma cases with sufficient follow-up data are needed to better illustrate the potential difference between the *BRAF* mutation status and recurrence in UAM and AM.

In our analyses, the *BRAF* V600E, *RAS, FGFR2*, and *SMO* were mutually exclusive in ameloblastoma. However, it has been reported in other diseases such as in squamous cell carcinoma of the head and neck that mutual exclusivity as well as co-occurrence of mutations may define a subgroup of the disease (The Cancer Genome Atlas Network 2015; Leemans et al. 2018). It is therefore tempting to hypothesize similar heterogeneity in AM, and a comprehensive analysis of the mutational spectrum could be of interest in UAM as well as in conventional AM.

In the present study, VE1 immunochemistry and molecular detection of the *BRAF* V600E mutations showed a high agreement in both the UAM and AM groups. Detection of the BRAF V600E mutation by VE1 immunohistochemistry has been reported to be 100% sensitive and specific in colorectal cancer and 100% sensitive and 96.8% specific in melanoma (Thiel et al. 2013, 2015), suggesting that VE1 immunochemistry performed on undecalcified tissue sections may be a valid surrogate for *BRAF* V600E genetic testing.

The morphologic classification of UAM is under debate, and we were hoping to add some clarity to it based on the mutations occurring in each subtype. Although this is the biggest cohort to analyze mutations in UAM so far, the small number of samples precluded the statistical analyses of the different mutations with histological subtypes. Moreover, analyses of copy number alterations and epigenetic changes in ameloblastoma will require further experimentation with a larger data set to strengthen the impact of BRAF V600E in this disease.

Conclusion

Our study demonstrates that *BRAF* V600E is the most common mutation in all 3 subtypes of UAM: luminal, intraluminal, and mural. We also show that *BRAF* V600E is slightly more common in UAM (94%) than in AM (74%) and that *RAS* and *FGFR2* mutations are found in AM but not in UAM. It may be concluded that dysregulation of the MAP-kinase pathway plays a critical role in the pathogenesis of both UAM and AM. It could therefore be argued that UAM and AM are part of a genetic as well as histomorphologic spectrum of the same odontogenic neoplasm. In light of the diagnostic and prognostic impacts of the mutation status, *BRAF* V600E analysis could be considered in routine ameloblastoma diagnostics.

Author Contributions

K. Heikinheimo, contributed to design, data acquisition, analysis, and interpretation, drafted and critically revised the manuscript; J.-M. Huhtala, A. Thiel, K.J. Kurppa, M. Kovac, K. Elenius, D. Baumhoer, A. Ristimäki, P.R. Morgan, contributed to design, data acquisition, analysis, and interpretation, critically revised the manuscript; C. Kragelund, G. Warfvinge, H. Dawson, H. Heikinheimo, contributed to data acquisition, analysis, and interpretation, critically revised the manuscript. All authors gave final approval and agree to be accountable for all aspects of the work.

Acknowledgments

The skillful technical assistance of Mariia Valkama (Institute of Dentistry, University of Turku) and Merja Haukka (University of Helsinki) is gratefully acknowledged. We are grateful to Juha Kettunen for the data acquisition and design of the tables and figures. The work was financially supported by the Maritza and Reino Salonen Foundation. The authors declare no potential conflicts of interest with respect to the authorship and/or publication of this article.

References

Benlloch S, Payá A, Alenda C, Bessa X, Andreu M, Jover R, Castells A, Llor X, Aranda FI, Massutí B. 2006. Detection of BRAF V600E mutation in colorectal cancer. J Mol Diagn. 8(5):540–543.

Bland JM, Altman DG. 2000. Statistics notes: the odds ratio. BMJ. 320(7247):1468.

Brown NA, Rolland D, McHugh JB, Weigelin HC, Zhao L, Lim MS, Elenitoba-Johnson KS, Betz BL. 2014. Activating *FGFR2-RAS-BRAF* mutations in ameloblastoma. Clin Cancer Res. 20(21):5517–5526.

Buhrman G, Holzapfel G, Fetics S, Mattos C. 2010. Allosteric modulation of Ras positions Q61 for a direct role in catalysis. Proc Natl Acad Sci USA. 107(11):4931–4936.

The Cancer Genome Atlas Network. 2015. Comprehensive genomic characterization of head and neck squamous cell carcinomas. Nature. 517(7536):576–582.

Cosmic (Catalogue of Somatic Mutations in Cancer) Database [accessed 2018 March 27]. http://cancer.sanger.ac.uk/cosmic/mutation/overview?id=216037.

Diniz MG, Gomes CC, Guimarães BV, Castro WH, Lacerda JC, Cardoso SV, de Faria PR, Dias FL, Eisenberg AL, Loyola AM, et al. 2015. Assessment of BRAFV600E and SMOF412E mutations in epithelial odontogenic tumours. Tumour Biol. 36(7):5649–5653.

Gomes CC, Diniz MG, Gomes RS. 2014. Progress towards personalized medicine for ameloblastoma. J Pathol. 232(5):488–491.

Heikinheimo K, Sandberg M, Happonen RP, Virtanen I, Bosch FX. 1991. Cytoskeletal gene expression in normal and neoplastic human odontogenic epithelia. Lab Invest. 65(6):688–701.

Heikinheimo K, Kurppa KJ, Laiho A, Peltonen S, Berdal A, Bouattour A, Ruhin B, Catón J, Thesleff I, Leivo I, et al. 2015. Early dental epithelial transcription factors distinguish ameloblastoma from keratocystic odontogenic tumor. J Dent Res. 94(1):101–111.

Heikinheimo K, Kurppa KJ, Elenius K. 2015. Novel targets for the treatment of ameloblastoma. J Dent Res. 94(2):237–240.

Holderfield M, Deuker MM, McCormick F, McMahon M. 2014. Targeting RAF kinases for cancer therapy: BRAF-mutated melanoma and beyond. Nat Rev Cancer. 14(7):455–467.

Kato S, Lippman SM, Flaherty KT, Razelle Kurzrock R. 2016. The conundrum of genetic "drivers" in benign conditions. J Natl Cancer Inst. 108(8):djw036.

Kim J, Aftab BT, Tang JY, Kim D, Lee AH, Rezaee M, Kim J, Chen B, King EM, Borodovsky A, et al. 2013. Itraconazole and arsenic trioxide inhibit Hedgehog pathway activation and tumor growth associated with acquired resistance to smoothened antagonists. Cancer Cell. 23(1):23–34.

Kurppa KJ, Catón J, Morgan PR, Ristimäki A, Ruhin B, Kellokoski J, Elenius K, Heikinheimo K. 2014. High frequency of BRAF V600E mutations in ameloblastoma. J Pathol. 232(5):492–498.

Leemans CR, Snijders PJ, Brankenhoff RH. 2018. The molecular landscape of head and neck cancer. Nat Rev Cancer. 18(5):269–282.

Li TJ, Wu YT, Yu SF, Yu GY. 2000. Unicystic ameloblastoma: a clinicopathologic study of 33 Chinese patients. Am J Surg Pathol. 24(10):1385–1392.

Pereira NB, Pereira KM, Coura BP, Diniz MG, de Castro WH, Gomez RS. 2016. BRAFV600E mutation in the diagnosis of unicystic ameloblastoma. J Oral Pathol Med. 45(10):780–785.

Rich JT, Neely JG, Paniello RC, Voelker CC, Nussenbaum B, Wang EW. 2010. A practical guide to understanding Kaplan-Meier curves. Otolaryngol Head Neck Surg. 143(3):331–336.

Richards S, Aziz N, Bale S, Bick D, Das S, Gastier-Foster J, Grody WW, Hegde M, Lyon E, Spector E, et al; ACMG Laboratory Quality Assurance Committee. 2015. Standards and guidelines for the interpretation of sequence variants: a joint consensus recommendation of the American College of Medical Genetics and Genomics and the Association for Molecular Pathology. Genet Med. 17(5):405–424.

Robinson L, Martinez MG. 1977. Unicystic ameloblastoma: a prognostically distinct entity. Cancer. 40(5):2278–2285.

Sweeney RT, McClary AC, Myers BR, Biscocho J, Neahring L, Kwei KA, Qu K, Gong X, Ng T, Jones CD, et al. 2014. Identification of recurrent *SMO* and *BRAF* mutations in ameloblastomas. Nat Genet. 46(7):722–725.

Therneau T. 2015. A Package for Survival Analysis in S, version 2.38 [accessed 2018 Aug 15]. https://CRAN.R-project.org/package=survival

Therneau TM, Grambsch PM. 2000. Modeling survival data: extending the Cox model. New York: Springer International.

Thiel A, Heinonen M, Kantonen J, Gylling A, Lahtinen L, Korhonen M, Kytölä S, Mecklin JP, Orpana A, Peltomäki P, et al. 2013. BRAF mutation in sporadic colorectal cancer and Lynch syndrome. Virchows Arch. 463(5):613–621.

Thiel A, Moza M, Kytölä S, Orpana A, Jahkola T, Hernberg M, Virolainen S, Ristimäki A. 2015. Prospective immunohistochemical analysis of BRAF V600E mutation in melanoma. Hum Pathol. 46(2):169–175.

Thomas BL, Sharpe PT. 1998. Patterning of the murine dentition by homeobox genes. Eur J Oral Sci. 106(Suppl 1):48–54.

Vered M, Muller S, Heikinheimo K, Ameloblastoma. In: El-Naggar AK, Chan JKC, Grandis JR, Takata T, Slootweg PJ, editors. 2017. World Health Organization classification of head and neck tumours. 4th ed. Lyon (France): IARC. p. 215–218.

Wright JM, Odell EW, Speight PM, Takata T. 2014. Odontogenic tumors, WHO 2005: where do we go from here? Head Neck Pathol. 8(4):373–382.